ADVANCES IN ATMOSPHERIC SCIENCES, VOL. 25, NO. 5, 2008, 856–866

Decadal and Interannual Variability of the Indian Ocean Dipole

YUAN Yuan*[1,2,3] (袁 媛), C. L. Johnny CHAN[2,4] (陈仲良), ZHOU Wen[2,4] (周 文), and LI Chongyin[1] (李崇银)

[1] *State Key Laboratory of Numerical Modeling for Atmospheric Sciences and Geophysical Fluid Dynamics, Institute of Atmospheric Physics, Chinese Academy of Sciences, Beijing* 100029

[2] *CityU-IAP Laboratory for Atmospheric Sciences, City University of Hong Kong, Hong Kong*

[3] *Graduate University of Chinese Academy of Sciences, Beijing* 100049

[4] *Department of Physics and Materials Science, City University of Hong Kong, Hong Kong*

(Received 13 August 2007; revised 21 February 2008)

ABSTRACT

This study investigates the decadal and interannual variability of the Indian Ocean Dipole (IOD). It is found that the long-term IOD index displays a decadal phase variation. Prior to 1920 negative phase dominates, but after 1960 positive phase prevails. Under the warming background of the tropical ocean, a larger warming trend in the western Indian Ocean is responsible for the decadal phase variation of the IOD mode. Due to reduced latent heat loss from the local ocean, the western Indian Ocean warming may be caused by the weakened Indian Ocean westerly summer monsoon.

The interannual air-sea coupled IOD mode varies on the background of its decadal variability. During the earlier period (1948–1969), IOD events are characterized by opposing SST anomaly (SSTA) in the western and eastern Indian Ocean, with a single vertical circulation above the equatorial Indian Ocean. But in the later period (1980–2003), with positive IOD dominating, most IOD events have a zonal gradient perturbation on a uniform positive SSTA. However, there are three exceptionally strong positive IOD events (1982, 1994, and 1997), with opposite SSTA in the western and eastern Indian Ocean, accompanied by an El Niño event. Consequently, two anomalous reversed Walker cells are located separately over the Indian Ocean and western-eastern Pacific; the one over the Indian Ocean is much stronger than that during other positive IOD events.

Key words: Indian Ocean dipole, ENSO, decadal phase variation, interannual variability

Citation: Yuan, Y., C. L. J. Chan, W. Zhou, and C. Y. Li, 2008: Decadal and interannual variability of the indian ocean dipole. *Adv. Atmos. Sci.*, **25**(5), 856–866, doi: 10.1007/s00376-008-0856-0.

1. Introduction

There exits a unique air-sea coupled mode termed the Indian Ocean Dipole (IOD; e.g., Saji et al., 1999; Webster et al., 1999) with opposing sea surface temperature anomaly (SSTA) in the western and eastern tropical Indian Ocean (TIO). Many studies have been published concerning its seasonal and interannual variability (e.g., Li et al., 2003; Saji and Yamagata, 2003a), its connection with the El Niño-Southern Oscillation (ENSO; e.g., Li et al., 2002; Ashok et al., 2003), and also its impacts on the climate in local and remote regions (e.g., Black et al., 2003; Saji and Yamagata, 2003b).

More recently, the decadal modulation of the IOD's impact on the global climate has received great attention. It is reported that the frequent occurrence of the IOD in last two decades of the twentieth century has reduced ENSO effects on the Indian summer monsoon rainfall (Ashok et al., 2001) and even weakened the link between El Niño and the Southern Oscillation (Behera and Yamagata, 2003). Furthermore, in studying the decadal correlations between the IOD mode and the winter monsoon rainfall over Southern India,

*Corresponding author: YUAN Yuan, yuanyuan@mail.iap.ac.cn

Kripalani and Kumar (2004) found a decadal variability of the seasonal mean IOD index during the last 130 years, which is characterized by an asymmetrical variation of its positive and negative phases. They also mentioned that the greenhouse warming may be a possible reason.

Ashok et al. (2004) proposed the existence of the decadal IOD variation with an 8–25-year period and suggested the involvement of the subsurface ocean dynamics. However, their data only covers the 1950–1999 period, and they mainly focused on the strength of the IOD, not the decadal change of IOD phases as noted by Kripalani and Kumar (2004). Based on the previous research, the present paper aims to answer two questions: (1) What are the physical mechanisms for the decadal phase variation of the long-term IOD mode? (2) Is there any difference of the interannual air-sea interaction associated with the decadal IOD?

The rest of the paper is organized as follows: section 2 describes the data and methodology. The decadal phase variation of the seasonal mean IOD index is then shown in section 3, and possible mechanisms are investigated in section 4. Section 5 reports the interannual air-sea coupled IOD mode on the background of its decadal variability. Section 6 gives a summary and discussion.

2. Data and methodology

The atmospheric variables used in this study are monthly wind and latent heat flux data with a 56-year (1948–2003) period, which are derived from National Centers for Environmental Prediction/National Center for Atmospheric Research (NCEP/NCAR) reanalysis (Kistler et al., 2001). SST data mainly comes from the monthly Hadley Center sea ice and SST dataset (HadISST), with $1^\circ \times 1^\circ$ latitude/longitude resolution and a 134-year period of 1870–2003 (Rayner et al., 2003). The 20°C isotherm depth (D20) provided by the Simple Ocean Data Assimilation (SODA) dataset of 1950–2001 (Carton et al., 2000) is adopted to describe the thermocline variation in the subsurface ocean.

Interannual anomalies are obtained by deviations from the climatological cycle based on the individual timescale of each dataset. The IOD index is defined as SSTA difference between the western (10°S–10°N, 50°–70°E) and eastern (10°S–0°, 90°–110°E) Indian Ocean (Saji et al., 1999). Positive IOD or positive phase means warm (cool) in the west (east), and the opposite pattern is for negative IOD or negative phase. The seasonal mean (September–October–November: SON) IOD index is prepared as its peak usually occurs in the boreal autumn. The Niño3 index (SSTA area-averaged over 5°S–5°N, 150°–90°W) and the TIO index (SSTA area-averaged over 15°S–10°N, 45°–105°E) are also used to represent ENSO and the basin-wide SSTA variation in the TIO respectively.

A Fast Fourier Transform (FFT; Bingham et al., 1967) is applied to isolate decadal fluctuation. The ENSO signal is removed from the IOD index using $I_{\rm IODM} = I_{\rm AIODM} + r(I_{\rm IODM}, I_{\rm NINO3}) \cdot \sigma \cdot \tilde{I}_{\rm NINO3}$ (Ashok et al., 2003), where $\tilde{I}_{\rm NINO3}$ is the normalized Niño3 index ($I_{\rm NINO3}$), σ is the standard deviation (0.36°C) of the IOD index ($I_{\rm IODM}$), $r(I_{\rm IODM}, I_{\rm NINO3})$ denotes their correlation coefficient, and $I_{\rm AIODM}$ is the remainder of the $I_{\rm IODM}$ with the ENSO signal removed. $I_{\rm NINO3}$ can be replaced by the TIO index ($I_{\rm TIO}$) to remove the TIO signal from the IOD index.

The statistical significance of the correlation results is tested by the t-test

$$t = \frac{r\sqrt{N_{\rm dof} - 2}}{\sqrt{1 - r^2}} ,$$

in which the effective number of degrees of freedom is evaluated by:

$$N_{\rm dof} = N \frac{1 - r_1 r_2}{1 + r_1 r_2} ,$$

$N_{\rm dof}$ is the number of effective sample size, N is the sample size, and r_1 or r_2 is the one-lag autocorrelation for each time series (Bretherton et al., 1999).

Composite analyses are performed respectively on the positive and negative IOD events, which are selected based on the one standard deviation (0.36°C) of the IOD index during 1948–2003. The result significance is tested by using the classical Student's t-test (Chervin and Schneider, 1976).

3. Decadal phase variation of the IOD index

The normalized autumn (SON) IOD index exhibits an increasing linear trend and a prominent decadal phase variation (Fig. 1a). Negative phase dominates the earlier 1880–1919 period, while positive IOD occurs more frequently after 1960; during the transitional period (1920–1959), the dipole is inactive. To confirm such decadal variability of the IOD index, we have also examined two other SST datasets over 100 years: the extended reconstruction of global SST (ERSST) produced on Comprehensive Ocean-Atmosphere Data Set (COADS) from 1854 to 2005 (Smith and Reynolds, 2003), and the Kaplan SST data in 1856–2005 (Kaplan et al., 1998). Both of these show the same decadal phase variation of the index (not shown), confirming the recent findings by Kripalani and Kumar (2004; their Fig. 5) and Kulkarni et al. (2007; their Fig. 2), and also suggesting that the decadal fluctuation of the two phases should be an

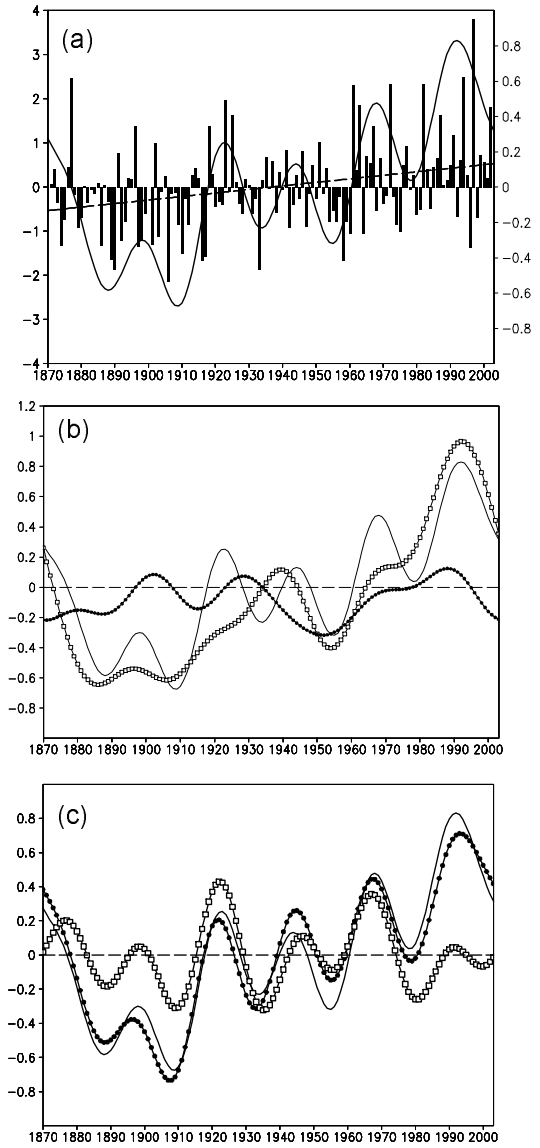

Fig. 1. (a) Time series of the normalized autumn (SON) IOD index (bar using the y-axis on the left), with its linear trend (dashed line) and decadal variability (solid curve; using the y-axis on the right). (b) Decadal IOD (solid curve; same as the curve in Fig. 1a), Niño3 (dots) and TIO (squares) index. (c) Decadal IOD (solid curve; same as the curve in Fig. 1a) index. Also shown are the decadal IOD index with ENSO signal removed (dots) and TIO signal removed (squares). All decadal indices are normalized by their individual standard deviation, and filtered by 21-year low-pass FFT.

important feature of the long-term IOD index.

4. Physical mechanisms

To explore the physical mechanisms for the decadal variation of IOD phase, we considered two possible factors: one is the external forcing by ENSO and the other is the internal influence from the background Indian Ocean SSTA.

ENSO is associated with a decadal manifestation (Nitta and Yamada, 1989), but Ashok et al. (2004) and Tozuka et al. (2007) have suggested that the time series of the decadal IOD and ENSO indices are not well correlated. In our analysis, the 21-year low-pass filtered Niño3 index also displays a dissimilar feature (dots in Fig. 1b) from that of the IOD index, with an insignificant correlation of -0.174 between them. Very little change occurs in the decadal IOD when ENSO signal is removed (dots in Fig. 1c), reaffirming that ENSO contributes little to IOD decadal variability.

On the contrary, the background TIO SSTA (as represented by the TIO index) exhibits a very similar decadal variability (squares in Fig. 1b) to the IOD index. When the TIO signal is subtracted from the IOD index, the original decadal phase variation of the latter almost disappears (squares in Fig. 1c).

Based on the zero line of the decadal IOD index (Fig. 1a), we divide the entire period into three epochs: 1880–1919, 1920–1959 and 1960–2003. By comparing the climatological mean SST in each epoch, it is identified that the warm pool region (as represented by the 28°C isotherm), which covers the eastern Indian Ocean and the western Pacific, is enlarging with time (not shown), reflecting a global warming trend in the tropical Indo-Pacific Ocean. Kripalani and Kumar (2004) have hypothesized that the greenhouse warming might be a cause for the decadal phase variation of the IOD mode. But the index is defined as the SSTA difference between the western and eastern Indian Ocean. If both poles had the same warming trend, it would be impossible for the IOD mode to change from negative phase to positive phase. Therefore, we extend their work by removing the mean linear trend of the SST averaged in the entire domain (30°S–30°N, 40°E–80°W) from the original data in each grid. After that, the SST differences between every two periods show positive values persistent in the western Indian Ocean, i.e., the western pole of the IOD index (Fig. 2). Especially in the difference diagram between the latest (1960–2003) and the earliest (1880–1919) period, this pole has an increase in SST as high as 0.4°C, while other regions have mostly negative values (Fig. 2c). Therefore, the global warming trend of the tropical ocean cannot completely explain the decadal phase variation of the IOD mode, whereas different warming intensity between the western and eastern Indian Ocean should play an important role.

We further compare the decadal variability of the autumn (SON) SSTA averaged at either pole of the IOD mode, respectively defined as west index and east

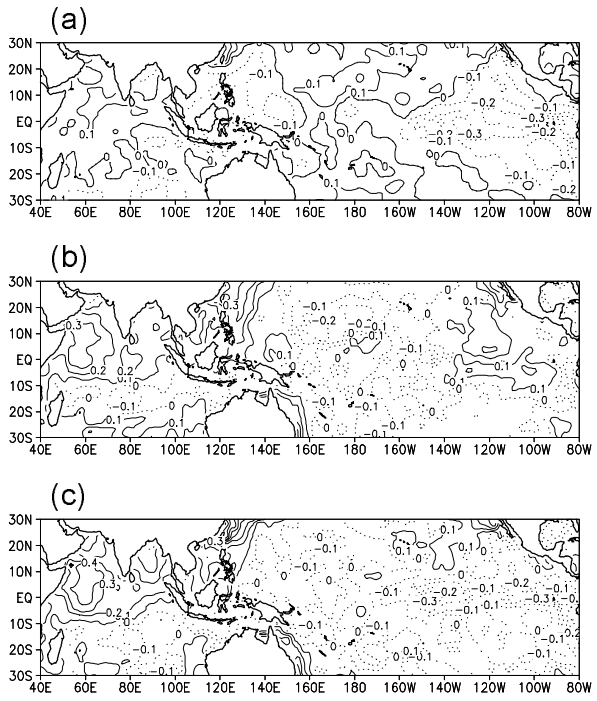

Fig. 2. SST differences between (a) 1920–1959 and 1880–1919, (b) 1960–2003 and 1920–1959, and (c) 1960–2003 and 1880–1919. Before that, the SST has been detrended using the area-averaged (30°S–30°N, 40°E–80°W) linear trend. Solid (dashed) curves are for positive (negative) values. Contour interval is 0.1°C.

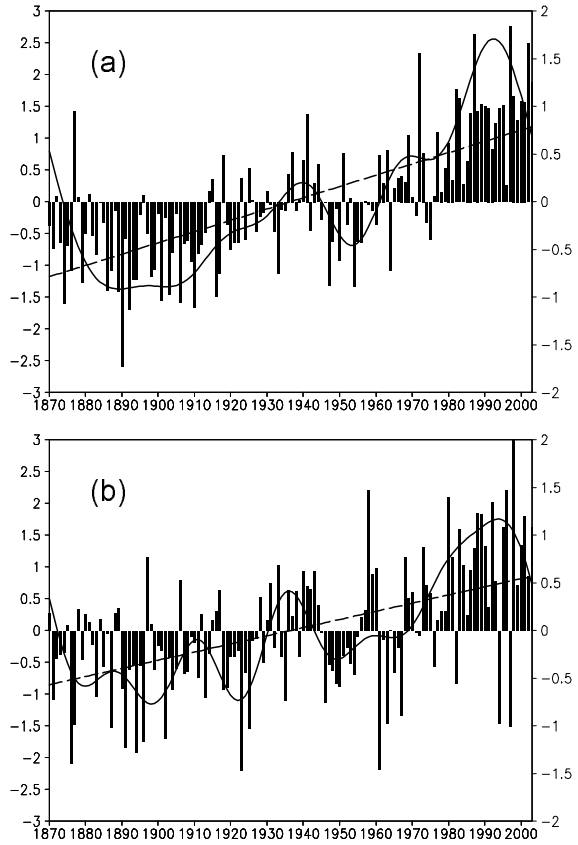

Fig. 3. Same as Fig. 1a, but for (a) west and (b) east index, respectively defined as autumn (SON) SSTA averaged over the western (10°S–10°N, 50°–70°E) and eastern (10°S–0°, 90°–110°E) Indian Ocean.

index. Similar to the IOD index (see Fig. 1a), both poles display an evident decadal variability and an increasing linear trend (Fig. 3). However, the most important thing is that the slope of the linear trend in the west index (about 1°; Fig. 3a) is different from that in the east one (about 0.7°; Fig. 3b). During the earlier period (1880–1919), negative SSTA controls both regions, but the averaged SSTA in the western Indian Ocean (−0.75°C) is more negative than that in the eastern part (−0.46°C). Under the background of the global warming, both regions experience a warming event. Then, during 1960–2003, they both have positive SSTA most of the time, but with the averaged SSTA in the western Indian Ocean (0.90°C) also larger than that in the eastern part (0.60°C). The different warming trend thus leads to a more rapid SST increase in the western Indian Ocean. As a result, positive IOD dominates its negative phase gradually (see Fig. 1). The decadal variation of IOD phases should therefore be attributed to the different warming intensity between the western and eastern Indian Ocean, in agreement with Kulkarni et al. (2007). Finally, the last question is: what is the cause for the larger warming in the western Indian Ocean?

Previous researchers have interpreted the formation of the IOD mode mainly through the Bejerknes feedback and the Asian monsoon-Indian Ocean interaction (e.g., Li et al., 2003; Fischer et al., 2005). It is suggested that the westerly summer monsoon along the equatorial Indian Ocean would cause upwelling at the eastern coast of Africa (Webster et al., 1999) and latent heat loss from the local ocean (Venzke et al., 2000), which in turn decrease the SST in the western Indian Ocean. Hence, an increased summer monsoon could enhance cooling on the sea surface, while a weakened monsoon may reduce the cooling or even generate a warming in the western pole. Such local air-sea interaction is well illustrated by the lagged correlation between the low-level anomalous zonal wind in June–July–August (JJA) and the west index (SON). A significant negative correlation is rightly situated in the northwestern Indian Ocean, accompanied by another significant positive center near Madagascar (Fig. 4a). These results indicate that warming in the western Indian Ocean during autumn would follow the low-level anomalous easterlies off eastern Africa and westerlies in the southern Indian Ocean in the previous summer,

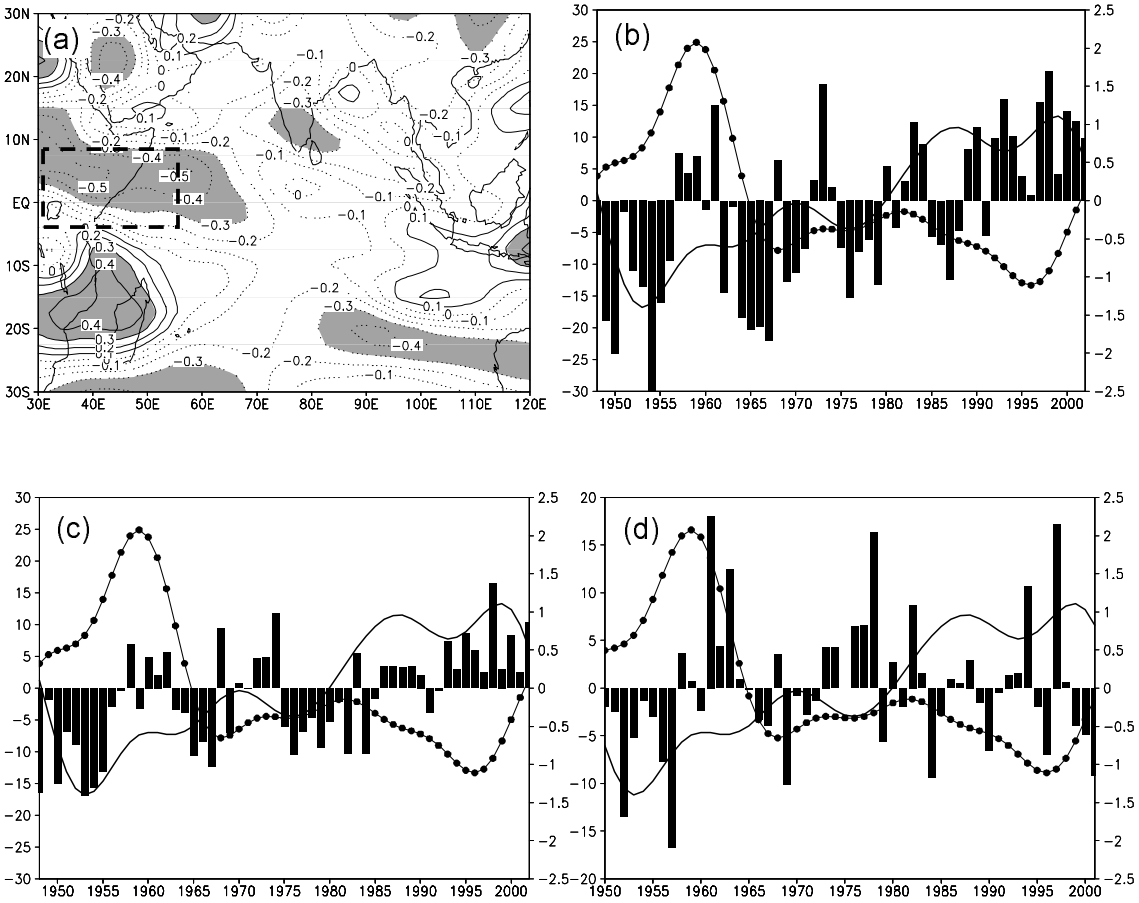

Fig. 4. (a) Correlations between 850-hPa anomalous zonal wind in summer (JJA) and the west index in autumn (SON). Shading indicates correlations significant above 95% confidence level. Time series of (b) summer (JJA) and (c) autumn (SON) latent heat flux anomalies (bar; W m^{-2}), and (d) autumn (SON) 20°C isotherm depth (bar; m) averaged in the western Indian Ocean (10°S–10°N, 50°–70°E), using the y-axis on the left. Also plotted are the normalized decadal (11-year low-pass filter) west (solid curve) and westerly (dots) indices, using the y-axis on the right. The westerly index is defined as summer (JJA) 850-hPa anomalous zonal wind averaged over 0°–10°N, 35°–60°E, indicated by the dashed box in Fig. 4a.

which is equivalent to a decreased monsoon circulation around the Indian Ocean.

To show the decadal variation of the Indian Ocean low-level monsoonal flow, a westerly index is defined as 850-hPa anomalous zonal wind in summer (JJA) averaged over the key region (0°–10°N, 35°–60°E; the dashed box in Fig. 4a). The decadal variability of this index displays a clear decadal transition from westerly anomalies to easterly anomalies around 1965 (dots in Figs. 4b–4d), confirming a weakening Asian summer monsoon during recent decades as documented by Wang (2001) and Xue (2001). More importantly, the decadal variation of the west index (solid curve in Figs. 4b–4d) is almost out of phase with that of the westerly index. Their significant negative correlation (−0.78) suggests that the weakening summer monsoon might be responsible for the warming in the western Indian Ocean.

Latent heat flux anomalies averaged over the western Indian Ocean (10°S–10°N, 50°–70°E) display a consistent variation with the west index, changing from mostly negative to positive values around the mid-1980s in both the summer (Fig. 4b) and autumn (Fig. 4c) seasons. Here, positive anomaly means the latent heat is lost from the ocean into the atmosphere, while negative anomaly means the opposite heat transmission. As shown in Fig. 4c, more latent heat released from the ocean during the latest ten years should be forced by the enhanced convection above the already warm western Indian Ocean (Guan et al., 2003). Similarly, the negative anomalies of the heat flux around the early 1950s can also be attributed to the suppressed convective activity above the coldest SSTA at the western pole. However, if negative heat flux anomalies persist, then the ocean would be warmed because of continuously reduced heat loss,

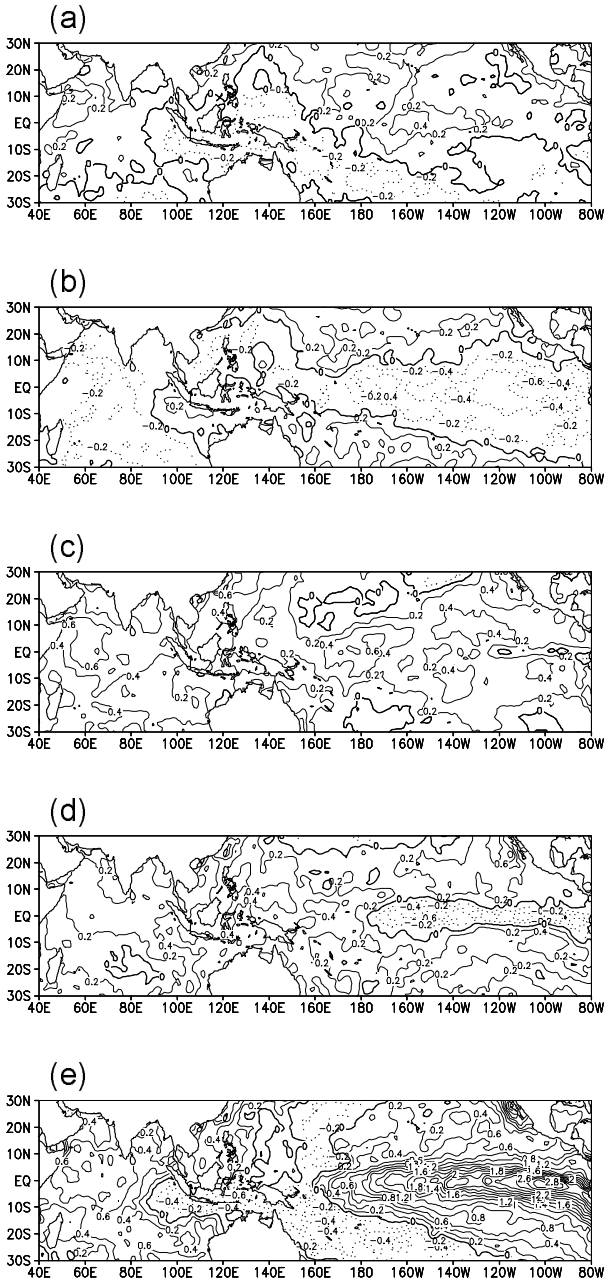

Fig. 5. Autumn (SON) SSTA structure composite for (a) positive and (b) negative IOD events during 1948–1969, for (c) positive (except 1982, 1994 and 1997) and (d) negative IOD events during 1980–2003, and also for (e) the three years of 1982, 1994 and 1997. Solid curves (dots) are for positive (negative) values, and the contour interval is 0.2°C.

which leads to a negative feedback of the atmosphere on the temperature variation in the local ocean. Meanwhile, the latent heat flux is also influenced by the low-level wind speed. When the climatological mean winds are intensified, more latent heat would be released from the ocean into the atmosphere; otherwise, less heat loss due to reduced wind speed would also help warming the ocean. As illustrated in Figs. 4b and 4c, negative latent heat anomalies with decreased westerly winds dominate from the 1960s to the 1980s, accompanied by the salient rising SSTA in the western Indian Ocean. Hence, less latent heat loss due to a previously cold sea surface and continuously reduced wind speed should provide the physical dynamics for the warming in the western Indian Ocean.

5. Interannual Indian Ocean Air-sea interaction in different decades

Under the background of the decadal variability of the IOD mode, we will investigate SSTA structure and three-dimensional atmospheric circulations, composite for positive and negative IOD events in different decades. Considering the shorter timescale of the available wind data and the reliability of the SST data, IOD events during 1948–2003 will be our focus. Table 1 lists all the extreme years based on one standard deviation (±0.36°C) of the IOD index. Two periods are examined according to its decadal variation (see Fig. 1a): the earlier period of 1948–1969 with positive and negative IOD fluctuating and the later period of 1980–2003 with positive IOD dominating. The period of 1970–1979 is not considered because of the so-called regime shift (e.g., Nitta and Yamada, 1989; Saji and Yamagata, 2003a).

During the earlier period (1948–1969), the SSTA structure composite for the positive IOD shows a "+ − +" pattern: warm in the western Indian Ocean, cold water from the eastern Indian Ocean to the western Pacific, and warm again in the central-eastern Pacific (Fig. 5a). A nearly reversed SSTA pattern "− + −" is for the composite negative IOD (Fig. 5b). If 0.5°C is set as the criteria for ENSO event, there is almost no ENSO signal in the eastern Pacific. Coupled to the positive IOD, surface easterly anomalies dominate the equatorial Indian Ocean and southeasterly winds are intensified along the western coast of Java (Fig. 6a). Meanwhile, two anomalous vertical cells can be identified above the equatorial Indo-Pacific Ocean: one over the Indian Ocean, and the other from the eastern Indian Ocean to the central Pacific, with the shared subsidence around the 110°E longitude (Fig. 6b). By contrast, coupled to the negative IOD which has the most negative SSTA over the central Indian Ocean (Fig. 5b), significant surface divergent flows occupy the central Indian Ocean (Fig. 6c). Along the equator, a single Walker cell prevails over the Indian Ocean, with anomalous downward motion in the central Indian Ocean and upward motion extending from the eastern Indian Ocean to the western Pacific (Fig. 6d).

Table 1. Positive and negative IOD events during the 1948–1969 and 1980–2003 periods. All the selected events are based on one standard deviation (±0.36°C) of the autumn (SON) IOD index (1948–2003).

1948–1969		1980–2003	
Positive IOD	Negative IOD	Positive IOD	Negative IOD
1949 1951 1953 1961 1962 1963 1965 1966 1967 1969	1954 1955 1956 1958 1959 1960 1964 1968	**1982** 1983 1985 1986 1987 1990 1991 1993 **1994 1997** 1999 2000 2002 2003	1980 1981 1984 1992 1996 1998

Note: The years 1982, 1994 and 1997 are in bold, as they are composited separately from the positive IOD group in 1980–2003.

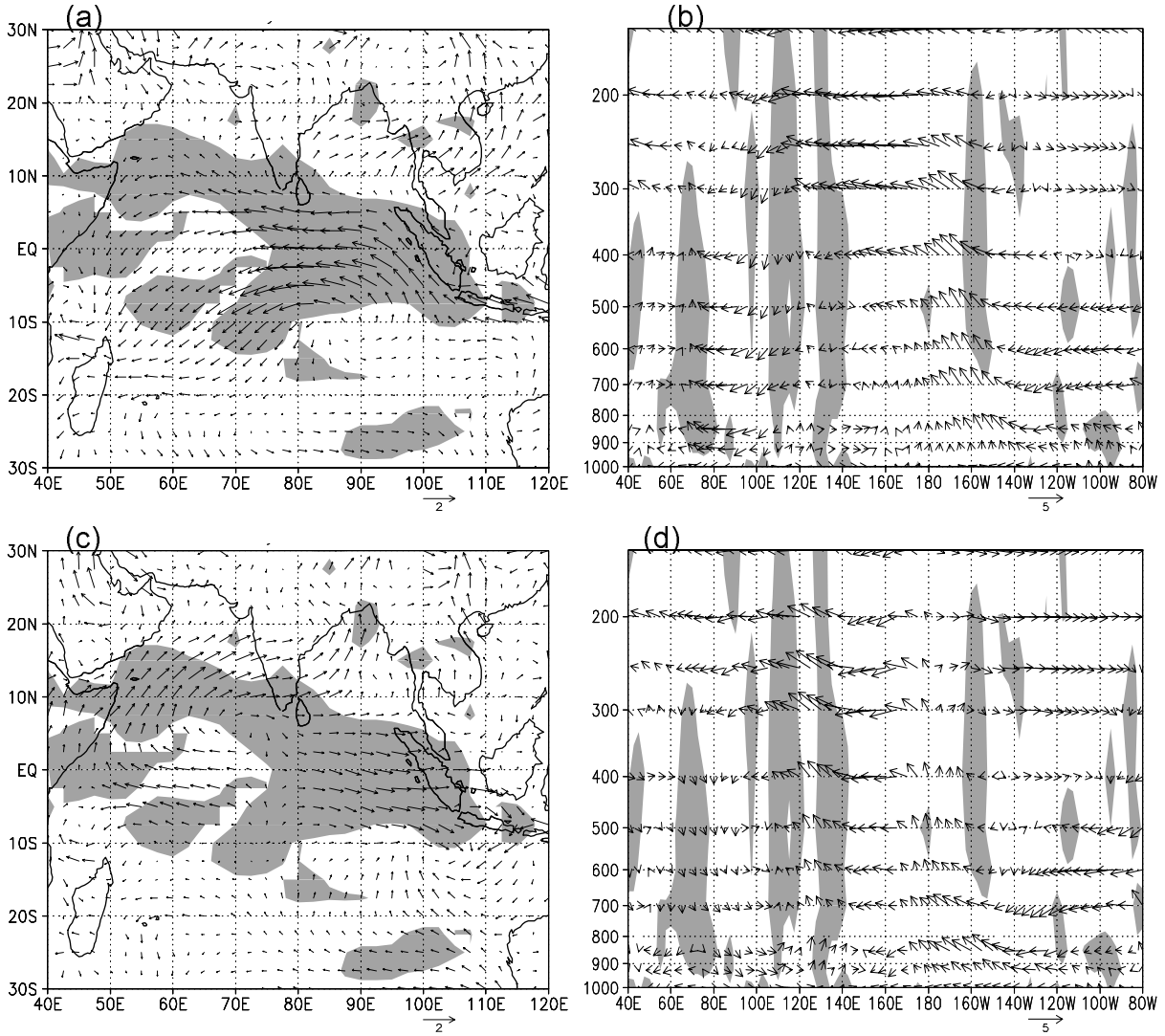

Fig. 6. Anomalous surface winds in autumn (SON) composite for (a) positive and (c) negative IOD during 1948–1969. Shadings indicate the zonal or meridional wind above the 95% confidence level. (b) and (d) are the same with (a) and (c) respectively, but for anomalous equatorial (5°S–5°N) vertical circulation in autumn (SON), with the vertical wind being multiplied by 100. Shadings indicate the anomalous vertical wind above the 95% confidence level. The y-axis in (b) and (d) shows the pressure height (units: hPa).

During the most recent period (1980–2003) except 1982, 1994 and 1997, both positive and negative IODs are featured as a zonal but opposite gradient perturbation on a uniform positive SSTA (Figs. 5c and 5d). No El Niño signal can be identified with the positive IOD, whereas a La Niña event is somewhat obvious in the composite of negative IOD. For positive IOD, the anomalous surface wind circulation in the Indian Ocean (Fig. 7a) is very similar to that of the earlier period (see Fig. 6a), but with a slightly decreased intensity. The anomalous vertical circulation is also reduced, with a rising motion over most of the central Indian Ocean, and subsidence above the Maritime continent around 120°E (Fig. 7b). For negative IOD, the surface winds are the reverse (Fig. 7c) of the positive condition except for the fact that two vertical cells are evident over the tropical Indian Ocean and western-central Pacific respectively, with a downward anomaly in the western Indian Ocean and central Pacific, and an upward anomaly in the eastern Indian Ocean around 110°E.

Finally, 1982, 1994 and 1997 are composited separately from the positive IOD group during 1980–2003 for the reason that only these three years have negative SSTA in the eastern Indian Ocean (see bars in Fig. 3b). The salient "+ − +" SSTA pattern reflects a co-occurrence of a positive IOD and an El Niño event (Fig. 5e), very similar to the structure in Fig. 5a, but being considerably intensified. Correspondingly, both the horizontal surface winds (Fig. 7e) and the equatorial vertical circulation (Fig. 7f) are significantly strengthened. Two anomalous reversed Walker Cells occupy the tropical Indian Ocean and the Pacific respectively. These results suggest the possible linkage between IOD and ENSO through a pair of coupled evolving Walker circulations (e.g., Li et al., 2002; Chao et al., 2005), and also indicate that the co-occurrence of an El Niño event could favor a stronger positive IOD mode with an increased surface circulation and an enhanced single vertical cell over the tropical Indian Ocean, substantiating the previous study by Saji and Yamagata (2003a).

6. Summary and discussion

The present study investigates the decadal and interannual variability of the IOD mode. In agreement with Kripalani and Kumar (2004), the seasonal stratified (SON) IOD index displays a decadal phase variation: during the 1880–1919 period, negative IOD dominates; but in the more recent 1960–2003 period, positive phase occurs more frequently. On the background of the global warming, most of the tropical ocean experiences a warming trend in the last 130 years. However, the larger warming in the western Indian Ocean should be responsible for the decadal change of IOD phases, consistent with Kulkarni et al. (2007). Considering the decadal variation of the Asian summer monsoon (e.g., Wang, 2001; Xue, 2001), it is further revealed that warming in the western Indian Ocean may be caused by the reduced latent heat loss from the local ocean due to the weakening westerly monsoon flow off eastern Africa. Ashok et al. (2004) have proposed subsurface ocean dynamics for the decadal variability of the IOD. But in our analyses, the variation of the 20°C isotherm depth (D20) is quite different from that of the SSTA and the anomalous zonal winds averaged over the western Indian Ocean (see Fig. 4d). Nevertheless, the D20 data provided by SODA might have quality problems due to sparse observation, although they are probably the only available dataset for describing thermocline variations over a long period. On the other hand, some modeling studies have recently suggested that the decadal IOD may be governed by Ekman heat transport related to the Mascarene high activities or the Indonesian Throughflow associated with ENSO (e.g., Annamalai et al., 2005; Tozuka et al., 2007).

Under the background of decadal IOD, we made composites of SSTA structure and three-dimensional atmospheric circulations for positive and negative IOD events during 1948–1969 and 1980–2003. In the earlier period (1948–1969) with positive and negative IOD fluctuating, a single vertical cell forms over the tropical Indian Ocean that is coupled to the opposite SSTA in the western and eastern Indian Ocean. By contrast, during the later period of 1980–2003 with positive IOD dominating, most of the IOD events are characterized by a zonal gradient perturbation on a uniform positive SSTA. Correspondingly, the anomalous Walker cell over the TIO is not very prominent for positive IOD, consistent with Tan et al. (2003). However, there are three extremely strong positive IOD events during this period: 1982, 1994 and 1997. With an El Niño event co-occurring over the eastern Pacific, these three events exhibit opposite SSTA in the western and eastern Indian Ocean, and two anomalously reversed Walker cells separately located above the Indian Ocean and western-eastern Pacific. This signifies the possible connection between the IOD and ENSO phenomena through the "atmospheric bridge" (e.g., Lau and Nath, 1996; Klein et al., 1999), and also confirms the enhanced air-sea coupled IOD mode by the concurrence of the ENSO event (e.g., Saji and Yamagata, 2003a).

As mentioned in the Introduction, previous studies have noticed the frequent occurrence of recent IOD events (Ashok et al., 2001; Behera and Yamagata,

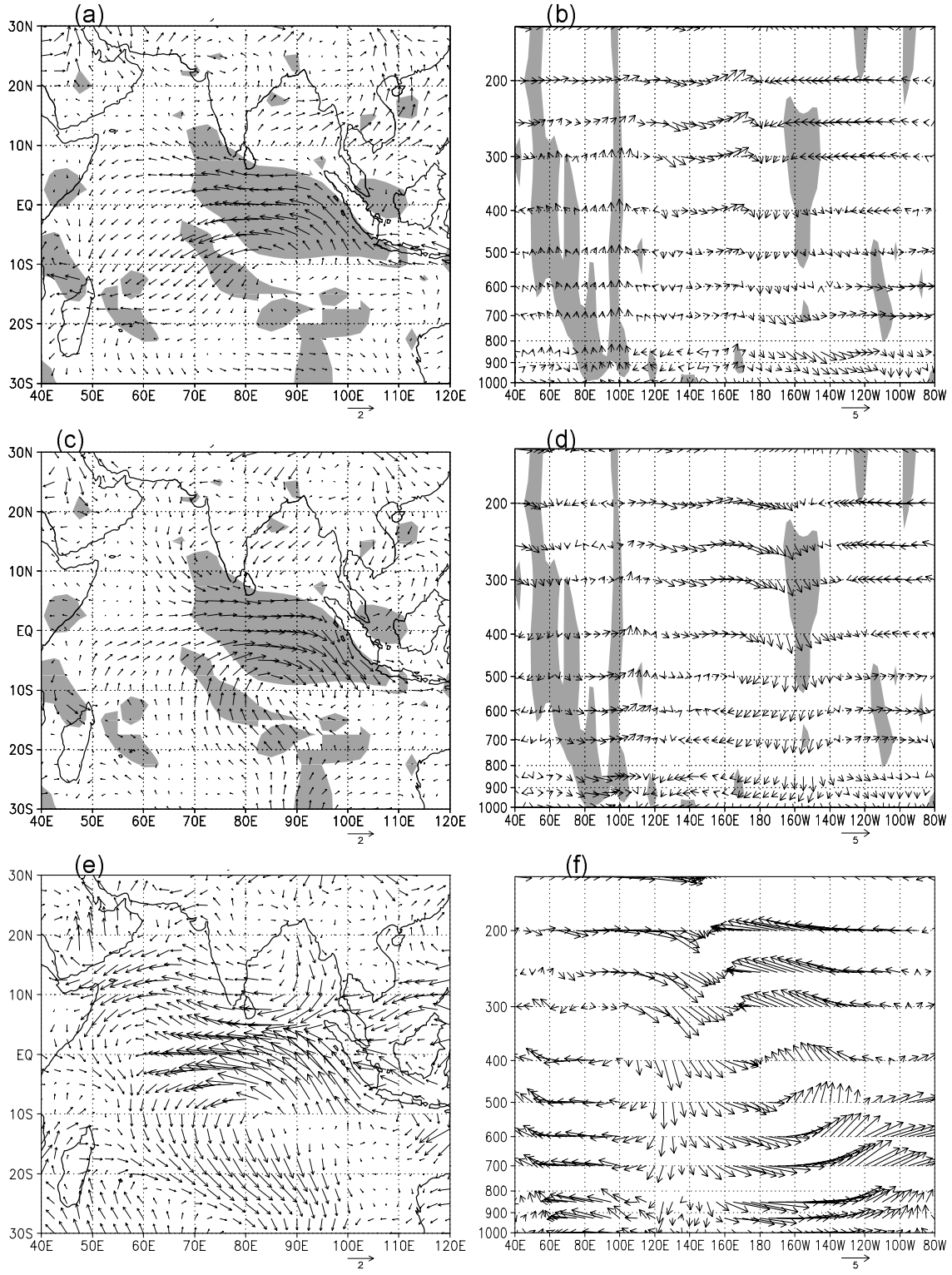

Fig. 7. Same as Fig. 6, but for (a) (b) positive IOD (except 1982, 1994 and 1997), (c) (d) negative IOD during 1980–2003, and (e) (f) 1982, 1994 and 1997. The y-axis in (b), (d) and (f) shows the pressure height (units: hPa).

2003; Annamalai et al., 2005). Li and Mu (2001) also stated that positive IOD is much stronger than the negative phase. However, considering the long-term IOD index, prior to 1920 it is the negative IOD that has a larger intensity and dominates over the positive one. Although Ashok et al. (2004) used outputs from a coupled general circulation model, their conclusion that there exists a strong decadal IOD signal in the late 1950s and 1960s, and again from the late 1980s to the 1990s is confirmed in our observation analyses, but with negative (positive) IOD dominating the earlier (later) period. Accordingly, except for the seasonal and interannual variability, such decadal phase variation should also be emphasized as another important characteristic of the IOD mode.

Acknowledgements. The authors acknowledge the support from the National Natural Science Foundation of China (NSFC; Grant No. 40675051) and the Innovation Key Program of the Chinese Academy of Sciences (Grant No. ZKCX2-SW-226). A large part of the work by the first author is completed as a joint collaborative work between City University of Hong Kong and the Institute of Atmospheric Physics, Chinese Academy of Sciences, and supported by City University of Hong Kong Research Grant 9610021.

REFERENCES

Annamalai, H., J. Potemra, R. Murtugudde, and J. P. McCreary, 2005: Effect of preconditioning on the extreme climate events in the tropical Indian Ocean. *J. Climate*, **18**, 3450–3469.

Ashok, K., Z. Guan, and T. Yamagata, 2001: Impact of the Indian Ocean dipole on the relationship between the Indian monsoon rainfall and ENSO. *Geophys. Res. Lett.*, **28**, 4499–4502.

Ashok, K., Z. Guan, and T. Yamagata, 2003: A look at the relationship between the ENSO and the Indian Ocean dipole. *J. Meteor. Soc. Japan*, **81**, 41–56.

Ashok, K., W. L. Chan, T. Motoi, and T. Yamagata, 2004: Decadal variability of the Indian Ocean dipole. *Geophys. Res. Lett.*, **31**, DOI: 10.1029/2004GL021345.

Behera, S. K., and T. Yamagata, 2003: Influence of the Indian Ocean dipole on the southern oscillation. *J. Meteor. Soc. Japan*, **81**, 169–177.

Bingham, C., M. D. Godfrey, and J. W. Tukey, 1967: Modern techniques of power spectrum estimation. *The Institute of Electrical and Electronics Engineeers Transaction on Audio and Electroacoustics*, **15**, 56–66.

Black, E., J. Slingo, and K. R. Sperber, 2003: An observational study of the relationship between excessively strong short rains in coastal East Africa and Indian Ocean SST. *Mon. Wea. Rev.*, **131**, 74–94.

Bretherton, C., M. Widmann, V. P. Dymnikov, J. M. Wallace, and I. Blade, 1999: The effective number of spatial degrees of freedom of a time-varying field. *J. Climate*, **12**, 1990–2009.

Carton, J. A., G. Chepurin, X. Cao, and B. Giese, 2000: A simple ocean data assimilation analysis of the global upper ocean 1950–1995. Part I: Methodology. *J. Phys. Oceanogr.*, **30**, 294–309.

Chao, J. P., Q. C. Chao, and L. Liu, 2005: The ENSO events in the tropical Pacific and dipole events in the Indian Ocean. *Acta Meteorologica Sinica*, **63**, 594–602. (in Chinese)

Chervin, R. M., and S. H. Schneider, 1976: On determining the statistical significance of climate experiments with General Circulation Models. *J. Atmos. Sci.*, **33**, 405–412.

Fischer, A. S., P. Terray, E. Guilyardi, S. Gualdi, and P. Delecluse, 2005: Two independent triggers for the Indian Ocean dipole/zonal mode in a coupled GCM. *J. Climate*, **18**, 3428–3449.

Guan, Z., K. Ashok, and T. Yamagata, 2003: The summertime response of the tropical atmosphere to the Indian Ocean sea surface temperature anomalies. *J. Meteor. Soc. Japan*, **81**, 533–561.

Kaplan, A., M. Cane, Y. Kushnir, A. Clement, M. Blumenthal, and B. Rajagopalan, 1998: Analyses of global sea surface temperature 1856–1991. *J. Geophys. Res.*, **103**, 567–589.

Kistler, R., and Coauthors, 2001: The NCEP-NCAR 50-year reanalysis: Monthly means CD-ROM and documentation. *Bull. Amer. Meteor. Soc.*, **82**, 247–268.

Klein, S. A., B. J. Soden, and N. C. Lau, 1999: Remote sea surface temperature variations during ENSO: Evidence for a tropical atmospheric bridge. *J. Climate*, **12**, 917–932.

Kripalani, R. H., and P. Kumar, 2004: Northeast monsoon rainfall variability over south peninsular India vis-a-vis Indian Ocean dipole mode. *International Journal of Climatology*, **24**, 1267–1282.

Kulkarni, A., S. S. Sabade, and R. H. Kripalani, 2007: Association between extreme monsoons and the dipole mode over the Indian subcontinent. *Meteorology and Atmospheric Physics*, **95**, 255–268.

Lau, N. C., and M. J. Nath, 1996: The role of the atmospheric bridge in linking tropical Pacific ENSO events to extratropical SST anomalies. *J. Climate*, **9**, 965–985.

Li, C. Y., and M. Q. Mu, 2001: The influence of the Indian Ocean dipole on atmospheric circulation and climate. *Adv. Atmos. Sci.*, **18**, 831–843.

Li, C. Y., M. Q. Mu, and J. Pan, 2002: Indian Ocean temperature dipole and SSTA in the equatorial Pacific Ocean. *Chinese Science Bulletin*, **47**, 236–239.

Li, T., B. Wang, C. P. Chang, and Y. Zhang, 2003: A theory for the Indian Ocean dipole-zonal mode. *J. Atmos. Sci.*, **60**, 2119–2135.

Nitta, T., and S. Yamada, 1989: Recent warming of tropical sea surface temperature and its relationship to the Northern Hemisphere circulation. *J. Meteor. Soc. Japan*, **67**, 375–383.

Rayner, N. A., D. E. Parker, E. B. Horton, C. K. Folland, L. V. Alexander, D. P. Rowell, E. C. Kent, and A. Kaplan, 2003: Global analyses of SST, sea ice and night marine air temperature since the late nineteenth century. *J. Geophys. Res.*, **108**(D14), 4407, DOI: 10.1029/2002JD002670.

Saji, N. H., and T. Yamagata, 2003a: Structure of SST and surface wind variability during Indian Ocean dipole mode years: COADS observations. *J. Climate*, **16**, 2735–2751.

Saji, N. H., and T. Yamagata, 2003b: Possible impacts of Indian Ocean dipole mode events on global climate. *Climate Research*, **25**, 151–169.

Saji, N. H., B. N. Goswami, P. N. Vinayachandran, and T. Yamagada, 1999: A dipole mode in the tropical Indian Ocean. *Nature*, **401**, 360–363.

Smith, T. M., and R. W. Reynolds, 2003: Extended reconstruction of global sea surface temperatures based on COADS data (1854–1997). *J. Climate*, **16**, 1495–1510.

Tan, Y. K., R. H. Zhang, and J. H. He, 2003: Features of the interannual variation of sea surface temperature anomalies and the air-sea interaction in tropical Indian Ocean. *Chinese J. Atmos. Sci.*, **27**, 53–66. (in Chinese)

Tozuka, T., J. J. Luo, S. Masson, and T. Yamagata, 2007: Decadal modulations of the Indian Ocean dipole in the SIMTEX-F1 coupled GCM. *J. Climate*, **20**, 2881–2894.

Venzke, S., M. Latif, and A. Villwock, 2000: The coupled GCM ECHO-2. Part II: Indian Ocean response to ENSO. *J. Climate*, **13**, 1371–1383.

Wang, H. J., 2001: The weakening of the Asian monsoon circulation after the end of 1970's. *Adv. Atmos. Sci.*, **18**, 376–386.

Webster, P. J., A. M. Moore, J. P. Loschnigg, and R. R. Leben, 1999: Coupled ocean-atmosphere dynamics in the Indian Ocean during 1997–98. *Nature*, **401**, 356–360.

Xue, F., 2001: Interannual to interdecadal variation of East Asian summer monsoon and its association with the global atmospheric circulation and sea surface temperature. *Adv. Atmos. Sci.*, **18**, 567–575.